Origin of boson peak in glasses: Role of atomic soft-mode excitations

M. I. Klinger* and L. Vatova
Department of Physics, Bar-Ilan University, Ramat-Gan 52900, Israel
(Received 9 July 2004; revised manuscript received 12 July 2005; published 28 October 2005)

In the present article, glasses are considered, for which THz frequency vibrational anomalies include both an experimentally observed boson peak and, above it, a "high-frequency" sound with well-defined acousticlike excitations. The phenomena are strongly related to an Ioffe-Regel crossover from a weak inelastic scattering of interacting acoustic and soft-mode (nonacoustic) vibrational excitations to a strong scattering and to an associated hybridization of both types of excitations. A theoretical soft-mode-dynamics model of the anomalies, actually containing a single material parameter, is presented, which is complete in the sense that it takes into account both the Ioffe-Regel crossover and a recently found "vibrational instability" effect due to elastic interactions between soft-mode vibrations. The basic vibrational density of states and the reduced density of states are calculated. The results appear to show that the qualitative features and scale estimations of the experimentally studied inelastic scattering intensities in the glasses under discussion can be described by the present complete soft-mode-dynamics model. The latter is compared with other recent theoretical models of the boson peak in glasses.

DOI: 10.1103/PhysRevB.72.134206 PACS number(s): 61.44.−n, 63.50.+x, 65.60.+a, 66.70.+f

I. INTRODUCTION

One of the general and well-known vibrational dynamic anomalies of glasses, at low frequencies $\nu \ll \nu_D$, is the boson peak (BP), a peak experimentally observed in inelastic photon (Raman, x-ray) and neutron-scattering intensities with the following qualitative and scale properties (ν_D is an effective Debye frequency). The BP is found at a THz scale frequency shift, $\nu = \nu_{BP} \equiv \omega_{BP}/2\pi \sim 1$ THz $\approx 0.1\nu_D$, and is asymmetric and broad with an effective half-width $\gamma_{BP} \approx \nu_{BP}$, while its temperature (T) dependence is described by a boson factor.[1] Then, in general, the origin of BP in a glass, for both the photon-inelastic-scattering and neutron-inelastic-scattering processes, is commonly assumed to be related to "scatterers" being harmonic low-frequency vibrational excitations. In the present article, the general theoretical soft-mode model of vibrational excitations of glasses (Sec. II, e.g., see Ref. 2) is applied to those probably including SiO_2, for which the THz frequency scale vibrational dynamic anomalies observed experimentally in the inelastic scattering spectra include both the BP and, above it, a correlated high-frequency sound (HFS) with well-defined acousticlike excitations observed at least in x-ray and neutron scattering.[3] Qualitative and scalewise properties of vibrational excitations found in the theoretical model presented are compared in what follows (Sec. IV) with experimental data for scattering intensities by applying well-known phenomenological relationships hardly dependent on specific features of models. Moreover, the dynamic (and thermal) anomalies of glasses occur at low frequencies $\nu \equiv \omega/2\pi \lesssim \nu_M \approx 2-3$ THz ($\ll \nu_D \approx 10$ THz, the Debye frequency) and/or $T \lesssim T_M \approx 100-150$ K ($\ll T_D$), being, in general, related to extra, non-Debye excitations of low frequencies, $h\nu \lesssim h\nu_M \approx (1-2)\times 10^{-2}$ eV ($\ll h\nu_D$).[1,3] Unlike the anomalies at very low $T \lesssim T_m \sim 1$ K and $\nu < \nu_m \sim 0.1$ THz determined by nonvibrational tunneling excitations,[1] the anomalies at moderately low T, $T_m < T \lesssim T_M \approx 100-150$ K, are assumed to be due to extra vibrational excitations of moderately low energies $h\nu$, $h\nu_m \approx 0.1$ meV $< h\nu < h\nu_M$.

It does not seem that a consistent microscopic approach and a quantitative theory of the BP in glasses are available at present (see Ref. 4). However, three different theoretical models—the mode-coupling model,[5,6] the soft-mode-dynamics (SMD) model[7] and the Euclidean random matrices approach[8]—have recently been proposed for describing the vibrational dynamic anomalies, as well as the associated thermal anomalies,[9] in the glasses under consideration (for a qualitative comparison of the models see Sec. V). All these models can be considered as "mean-field" models,[4] in the sense that each contains both microscopic model and phenomenological approximations, with a quantitative analysis based on real calculations, which together give rise to a qualitative (and probably a scalewise), rather than a quantitative description of the phenomena and their origins. The mentioned models appear to imply, in a sense, that the dynamic anomalies of a glass are associated with the existence of nonacoustic harmonic vibrational excitations interacting with the acoustic phonons of low frequencies. Unlike the models in Refs. 5, 6, and 8, in the original soft-mode-dynamics model of a glass,[7] the nonacoustic excitations are identified as harmonic vibrational excitations of atomic soft-mode "defects" (soft modes, in what follows). Moreover, the origin of the correlated BP and HFS is explicitly attributed to the phenomenon of the so-called Ioffe-Regel crossover from a standard weak-inelastic scattering of the phonons to an essentially different strong scattering, giving rise to a strong hybridization of acoustic phonons with harmonic vibrational soft-mode excitations. Another difference is that only in the soft-mode model nonvibrational tunneling excitations, determining the anomalies at very low T and ν, and nonacoustic vibrational excitations of moderately low energies are strongly correlated due to their common soft-mode origin.

The original concept of an Ioffe-Regel crossover (IRC)[10] from a weak scattering of acoustic phonons of wavelength λ_{ac}, with a mean-free path $l_{ac} \gg \lambda_{ac}$, to a strong scattering at

$l_{ac} \approx \lambda_{ac}$ at which the wave vector became no longer a good quantum number, was introduced for an elastic scattering from a static disorder in a crystal containing defects (or an amorphous solid). At present, however, an IRC can be considered as a general phenomenon for excitations for which a weak scattering is described by standard perturbation-theoretical expansions in the small parameter $\lambda_{ac}/l_{ac} \ll 1$, with terms $\propto (\lambda_{ac}/l_{ac})^n$ $(n=0,1,2\ldots)$, while the crossover to a strong scattering corresponds to $\lambda_{ac}/l_{ac} \approx 1$, so the expansion parameter is no longer small and the standard perturbation theory becomes irrelevant. In fact, a disordered system may contain both a static disorder and a "dynamic" disorder due to defects with proper (e.g., harmonic) vibrations, like those with "resonant" low-frequency harmonic vibrations in disordered crystals[11,12] or soft-mode defects in glasses. Thus, an IRC can occur at $\lambda_{ac}/l_{ac} \approx 1$ for either elastic or inelastic scattering.

The purpose of this article is to describe the complete soft-mode-dynamics model of the vibrational THz frequency scale anomalies and to reveal the underlying essential phenomenon—the IRC for inelastic scattering—in the glasses. The model is complete in the sense that it includes both the original soft-mode-dynamics model for the correlated BP and HFS, which account for the phenomenon of strong hybridization of acoustic phonons with vibrational soft-mode excitations in the IRC,[7] and the recently found effect of vibrational instability of low-frequency soft modes due to elastic interactions of the soft modes with each other.[13] The physical assumptions introduced earlier in the general theoretical soft-mode model (e.g., see Ref. 2) for understanding the origin of the soft modes are explained in Sec. II. In Sec. II, a brief review is also given of the soft-mode model of glasses and of the related original soft-mode-dynamics model, as well as of the model of the vibrational instability effect. The complete model of the vibrational THz frequency scale anomalies in the glasses and its defining relationships and basic statements are presented in Sec. III. Section IV presents and discusses the main results of this model and their comparisons with appropriate experimental scattering data and shows that the basic physics of the model is essentially related to the IRC for inelastic scattering of acoustic phonons from the soft-mode vibrations while the vibrational instability effect may contribute to quantitative aspects less important in the theory under discussion. Section V suggests some conclusions concerning the vibrational THz frequency dynamic anomalies and gives a comparison of the soft-mode-dynamics model with the other two, recent models[5,8] and also with recent alternative models[14] of the BP accounting for (acoustic) phonons in a random static field of a disordered system and an IRC for elastic scattering. The comparison appears to give rise to a prediction of two "limit" types of the dynamic anomalies (and, in this sense, of glasses).

II. SOFT-MODE-DYNAMICS MODEL OF LOW-FREQUENCY VIBRATIONAL ANOMALIES: INDEPENDENT SOFT MODES. INTERACTIONS BETWEEN SOFT MODES

The general theoretical soft-mode model of dynamic and thermal anomalies of glasses is an analytical mean-field theory, which in the simplest approximation of independent (not interacting with each other) soft modes has been proposed in Ref. 15, developed in Ref. 16, and later discussed and extended in a series of papers (e.g., see Ref. 17). The main concept of the model was that two types of low-energy atomic motions and related excitations—namely of (i) propagating acoustic phonons of low frequencies $\nu \ll \nu_D$, involving the vast majority of atoms, and (ii) soft-mode excitations related to a minority of atoms of a relatively low concentration $c_{sm}(\ll 1)$ in special local configurations of a random atomic network—coexisted and interacted with each other, determining the anomalies of the low-energy dynamics of glasses. As usual, the acoustic phonons of long wavelength, $\lambda_{ac} \gg a_1$, in a macroscopic solid system (e.g., a glass) are identified as Debye excitations of an appropriate elastic continuum, neglecting the specific atomic structure (a_1 is the average atomic spacing). On the other hand, the soft-mode excitations are resonant or quasilocal states characteristic of vibrational defect-related excitations of low frequencies around those of the acoustic phonons[11,12] (see also Refs. 18 and 19); in the Anderson classification,[20] these states are nonlocalized or extended ones, although not propagating wavelike states.

The basic point of the soft-mode model concerning the physical origin of the soft modes was as follows: In a glass, one could expect the occurrence of large and rare anisotropic spatial fluctuations (defects) of local atomic configuration parameters (bond angles, dihedral angles, etc.) from average values in medium-range order structures with typical effective atomic spring constants $k \approx k_0 \approx 10$ eV/Å^2. Such local fluctuations, which were characterized by small effective spring constants $k(x_{sm}) \equiv k_{sm} \ll k_0$, just turned out to be essential in the glass low-energy atomic dynamics. Indeed, it was shown in the soft-mode model that the most probable motion of atoms in such a local defect was going on along a single soft mode x_{sm} (dimensionless in atomic length $a_0 = 1$ Å) in an effective, practically quartic, anharmonic local potential $V_{sm}(x_{sm}) \simeq w(\eta_{sm} x_{sm}^2 + \xi_{sm} x_{sm}^3 + x_{sm}^4)$. Here η_{sm} and ξ_{sm} are the basic random (dimensionless) "softness" $(\eta_{sm} \gtrless 0)$ and asymmetry $(\xi_{sm} \lessgtr 0)$ parameters in a tail of a proper broad distribution density $F(\eta_{sm}, \xi_{sm})$ at $\{|\eta_{sm}|, \xi_{sm}^2\} \ll 1$ and $k \ll k_0$ (e.g., for $k \approx k_0 |\eta_{sm}|$), while w stands for the lowest vibrational excitation energy, $w \sim 1$ meV (e.g., see some reviews in Ref. 2). Although, in general, the effective mass μ_{sm} of a soft mode is a random parameter, its distribution density appears to be narrow so the parameter may be replaced by its average value $\mu_{sm} \approx (3-5)\mu_{av}$, with μ_{av} being an average atomic mass.

It was shown in this theory that the soft-mode excitations were anharmonic, nonvibrational, tunneling states for very low-excitation energies $h\nu' < h\nu_m \equiv w$ at $\nu_m \sim 0.1$ THz, while they were vibrational excitations at moderately low energies, $w < h\nu' \lesssim h\nu_{sm} (\ll h\nu_D)$; for soft-mode frequencies, the typical upper limit $\nu_{sm} \approx 0.1\nu_D$. Moreover, the majority of the vibrational excitations, in particular the THz frequency scale vibrational ones under consideration, were shown to be practically harmonic at $\nu_m < \nu' \lesssim \nu_{sm}$, with $V_{sm}(x_{sm}) \simeq w\eta_{sm} x_{sm}^2$ at $0 < \eta_{sm} \ll 1$. According to some experimental data, macroscopic disordered systems—in which no glassy

dynamic anomalies at very low temperatures and, thus, no tunneling states are observed—do not exhibit a BP in their scattering spectra.[21] This finding appears to show a strong correlation between the tunneling dynamics and harmonic vibrational excitations and, thus, supports the relevance of the soft-mode model for understanding the origin of the low-frequency dynamic and low-temperature thermal vibrational anomalies in glasses.

The interaction energy $V_{ac\text{-}sm}(x_{sm})$ of acoustic vibrations of a standard small elastic strain $e_{ac}(\ll 1)$ with a soft mode can be approximated in the most simple way by a direct harmonic coupling $V_{ac\text{-}sm}(x_{sm}) \approx \beta x_{sm} e_{ac}$. It is argued in the soft-mode model[2,17] that the random (scalar, for the sake of simplicity) coupling parameter β is subject to a narrow distribution function, so it may be well approximated by the related average value of a typical scale estimated as $|\beta| \approx 1$ eV$(\gg h\nu_D)$. It is also estimated in the general soft-mode model that a typical low-atomic concentration of the soft modes is appreciable, $c_{sm} \sim 10^{-2}$, and suggested for independent soft-mode defects that the "bare" harmonic vibrational excitations are characterized by a power-law density of states (DOS) $g_{sm}^{(0)}(\nu') = C_{sm}\nu_0^{-1}(\nu'/\nu_0)^{\alpha}$ normalized to unity with the constant $C_{sm} \propto c_{sm}^{-1}$. The DOS increases with the increase of the vibration frequency ν and contains two material parameters, namely, the typical soft-mode frequency, $\nu_0 \sim 1$ THz or $\nu_0 \approx 0.1\nu_D \lesssim \nu_{sm}$ and the exponent α varies in the range $2 \leqslant \alpha \leqslant 4$ depending on the shape of the soft-mode distribution density $F(\eta_{sm}, \xi_{sm})$ (e.g., see Ref. 2).

Recently, a mean-field model of soft-mode vibrational excitations and their DOS has been proposed,[13] which accounted for a renormalization of the bare quasilocal harmonic excitations of low frequency, $\nu' \ll \nu_c$ due to their (anharmonic) elastic interactions of energy $V_{12} = I_{12} x_{sm}^{(1)} x_{sm}^{(2)}$ with much more numerous vibrations of higher frequencies $\nu' \approx \nu_c$. Here, $|I_{12}| \sim J r_{12}^{-3}$ for a random distance r_{12} in a pair of soft modes with an effective strength parameter J and the frequency parameter ν_c was assumed to be substantially lower than the Debye one, $\nu_c \ll \nu_D$ (the many-body problem was approximated by the one for pairs of interacting soft-mode vibrations). The anharmonic interactions gave rise to structural relaxations and finally to reconstructed harmonic soft-mode oscillators of which the renormalized reduced DOS was calculated. The problem for a pair with bare frequencies ν_1' and ν_2', effective soft-mode masses $\mu_{sm}^{(1)} \approx \mu_{sm} \approx \mu_{sm}^{(2)}$, and the elastic interaction energy V_{12} was readily solved, giving rise to renormalized eigenfrequencies $(\nu_{\mp}')^2 = (\frac{1}{2})[(\nu_1'^2 + \nu_2'^2) \mp \sqrt{(\nu_1'^2 - \nu_2'^2)^2 + 4I_{12}^2[\mu_{sm1}\mu_{sm2}]^{-1}}]$ which, as well as the parameter ν_c, are random variables with some suggested distribution densities. Then, a vibrational (harmonic) instability occurs in the usual sense that $\nu_-'^2 < 0$ when $|I_{12}| > I_c \sim \nu_1'\nu_2'\sqrt{\mu_{sm1}\mu_{sm2}}$. It is worth mentioning in this connection the major result of the general soft-mode theoretical model (e.g., see Ref. 2): unstable harmonic motion modes exist in a disordered structure due to relatively large and rare structure fluctuations, and the stabilization of these modes is due to quartic anharmonicities. In the mean-field theory under consideration, the quartic anharmonicities are also taken into account for stabilizing the unstable harmonic soft modes. The frequency DOS of stabilized modes of low frequencies $\nu_s' \ll \nu_c$, at $\nu_s'^2 > 0$, was found to be linear, $g(\nu_s') \sim \nu_s'$, if the distribution of the random parameter I_{12} is smooth. Furthermore, interactions between the stabilized low-frequency soft-mode oscillators have approximately been taken into account and found to give rise to renormalized frequencies ν_r' of the resulting stable harmonic vibrations. The expression of the reduced DOS for the renormalized vibrations of low frequencies $\nu_r' \ll \nu_c$ calculated in this vibrational instability model has been found to contain a single material parameter, a characteristic vibration frequency ν^* determined by the effective strength parameter of the pair interactions

$$g^*(\nu_r')/\nu_r'^2 \propto (1/\nu^{*3})(\nu_r'/\nu^*)^2 \int_0^1 \frac{dz}{[1 + (\nu_r'/\nu^*)^6 z^2(3 - 2z^2)]}. \tag{1}$$

With increasing ν_r', the reduced DOS $g^*(\nu_r')/\nu_r'^2$ was found to increase like $\nu_r'^2$ at lower $\nu_r' < \nu_b$, while to decrease like $(\nu_r')^{-1}$ at higher $\nu_r' > \nu_b$, so that the reduced DOS exhibited a broad peak at $\nu_r' = \nu_b \simeq 1.1\nu^*$ (see Fig. 1 of Ref. 13) in which it was also assumed that a BP could be identified with this broad peak, i.e., $\nu_{BP} = \nu_b$. However, the related basic vibrational DOS $J^*(\nu_r'^2) = g^*(\nu_r')/2\nu_r'$ exhibits a plateaulike behavior instead of a peak (see Sec. IV), while the frequency DOS $g(\nu)$ monotonously increases with increasing ν (with only their slopes changing at $\nu = \nu^*$), at least up to frequencies $\nu \approx \nu_0$, a typical frequency of independent soft-mode vibrations. Taking into account the above, a conclusion is made in Sec. IV that Eq. (1) is hardly sufficient for a complete description of the BP and associated vibrational anomalies in the glasses under consideration.

Based on the general soft-mode model, the theoretical SMD model of the vibrational THz frequency dynamic vibrational anomalies in the glasses under discussion[7] is an analytical mean-field theory that approximates the glass for essential long-wave acoustic phonons by a three-dimensional (3D) isotropic elastic continuum containing randomly immersed independent localized defects, atomic soft modes which are characterized by low THz scale frequencies $\nu' (\lesssim \nu_{sm} \ll \nu_D)$ of harmonic vibrations. For the sake of simplicity, the scalar approximation is also used in this model, which does not distinguish longitudinal and transverse acoustic phonons. The purpose of the model was to calculate and discuss the resulting basic single-excitation DOS of harmonic vibrational excitations in a macroscopic-3D-disordered system of acoustic phonons which interact with independent harmonic soft-mode oscillators in the original SMD model. The problem under discussion in the SMD model is similar to that of the theory of vibrational spectra in a macroscopic-disordered-3D-crystalline lattice containing a finite atomic concentration c_d of randomly located quasilocal defects, or defects with quasilocal vibrational excitations; the concentration is low in the usual sense, $c_d \ll 1$, but can be "high" in a sense defined below.[18,19] Then, the SMD model can be developed as an appropriate extension of this theory to the abovementioned elastic continuum with immersed randomly located soft modes. The problem is not only to derive the dispersion law of the frequency spectrum for given real-

izations of the random harmonic system depending on the defect (e.g., soft mode) random parameters, but even more to find the basic macroscopic spectral properties (averaged over all realizations, i.e., macroscopic ensembles of random defect locations) which do not depend on random microscopic fluctuations.

The fundamental result of the theory[18,19] is that macroscopic spectral properties like the basic vibrational DOS $J(\varepsilon=\nu^2)=g(\nu)/2\nu$ and the related frequency DOS $g(\nu)$ are so-called self-averaging properties, being measurable macroscopic characteristics of the systems, which can practically be calculated by averaging the respective microscopic characteristics over all realizations. The calculations of the self-averaging DOS can be performed only for "long-wave" acoustic phonons, of which wavelengths overlap large numbers ($\gg 1$) of defects in mesoscopic subvolumes characterized on average by spatial homogeneity. The range of validity of the theory is determined by the criterion of "long-wave" acoustic excitations: the typical wavelength $\lambda_{ac}(\nu_0)=s_0\nu_0^{-1}\gg R_{av}=a_1c_d^{-1/3}$ (R_{av} is the mean separation of the defects, a_1 denotes the mean atomic separation, e.g., $a_1\approx 3$ Å). For often-studied defects (e.g., heavy-isotope ones) in a crystalline lattice, the resulting spectra of the vibrational excitations are explicitly found to be essentially different in two diverse ranges of c_d, "low" $c_d\ll c_0$ and high $c_d, c_0\ll c_d$ ($\ll 1$). The characteristic value c_0 of c_d can be defined from the equation $R_{av}(c_0)=\lambda_{ac}(\nu_0)$, so that $c_0=(\nu_0/\nu_D)^3$; here $\nu_D=s_0a_1^{-1}$ and s_0 is a typical (average) sound velocity. Moreover, the limit case of high concentrations just defines the range of validity of the theory that holds true for any kind of quasilocal defects, in particular, for the soft-mode defects. For the latter, the limit case of high concentrations is the only important one, because the typical low-atomic soft-mode concentration is $c_{sm}\approx 10^{-2}\gg c_0\approx 10^{-3}$ at the typical frequency $\nu_0\approx 0.1\nu_D$. Since the bare soft-mode vibrational excitations are characterized by a direct harmonic interaction with acoustic phonons, an inelastic (resonant) scattering of acoustic phonons from the soft-mode vibrational excitations occurs at $\nu_{ac}(q)=s_0q/2\pi\simeq\nu'$; q stands for an acoustic wave vector magnitude, $q\ll q_D\equiv 2\pi\nu_D/s_0$.

For the SMD model under discussion, as well as for the vibrational dynamics in disordered lattices, the basic vibrational DOS $J(\varepsilon)=\pi^{-1}\,\mathrm{Im\,Tr}\,G_{av}(\varepsilon)$ normalized to unity in what follows, and $G_{av}(\varepsilon)$ can be found by calculating the time (t) Fourier transform of $G_{av}(\mathbf{r}-\mathbf{r}';t)\equiv\langle G(\mathbf{r},\mathbf{r}';t)\rangle$, the system's single-excitation Green's function (for the continuum points $\mathbf{r},\mathbf{r}'$) averaged over all realizations, which is related in a standard way to the space-time correlators of the averaged acoustic and soft-mode displacements $(\mathbf{u}_{ac},x_{sm})$. For the latter, the equations of motion, as usual, can be established from the respective Lagrangian $L=K_{ac}+K_{sm}-V_{ac}-V_{sm}-V_{ac\text{-}sm}$ by applying the standard expressions of acoustic and (harmonic) soft-mode kinetic (K_{ac},K_{sm}) and potential (V_{ac},V_{sm}) energies and of the acoustic-soft-mode interaction energy $(V_{ac\text{-}sm})$. In the limit case of high $c_d=c_{sm}\gg c_0$, the Green's function approach can be applied for analytical calculations of $J(\varepsilon)$ as a power series in a small parameter, $\zeta\equiv R_{av}^3(c_{sm})\lambda_{ac}^{-3}(\nu_0)=c_0/c_{sm}\ll 1$, in which the basic contribution to the calculated quantities is determined by the lowest-order finite term. As usual, the approach is considered to be a well-founded consistent perturbation-theoretical one valid for $c_0\ll c_{sm}\ll 1$, of which the accuracy is controlled by small corrections relative to the main term, as ζ or smaller.

The defining equations of the theoretical SMD model under consideration contain both the equations of motion for the acoustic and soft-mode displacements $(\mathbf{u}_{ac},x_{sm})$ and the general relationship for the basic vibrational DOS, $J(\varepsilon)$. The equations of motion can be obtained, following the approximate Green's function method.[18,19] In particular, one has to replace the sum $\Sigma_{\mathbf{R}}\beta x_{sm}(R)e_{ac}(R)$, describing in the effective Hamiltonian the interactions of randomly located ($\mathbf{R}$) soft modes (in the continuum) with acoustic phonons, by the appropriate term $c_{sm}\beta x_{sm}e_{ac}$ that results from averaging expressions containing such a sum over the spatially homogeneous subvolumes. Then, the equations of motion are (retaining the main terms in the small parameter ζ) as follows:

$$\rho\frac{\partial^2\mathbf{u}_{ac}}{\partial t^2}\simeq\rho s_0^2\nabla_{\mathbf{R}}^2\mathbf{u}_{ac}+c_{sm}\beta\frac{\partial x_{sm}}{\partial\mathbf{R}},\tag{2}$$

$$\mu_{sm}\frac{\partial^2x_{sm}}{\partial t^2}\simeq-\mu_{sm}\nu'^2x_{sm}-\beta e_{ac},\tag{3}$$

where ρ is the average mass density of the elastic continuum and $e_{ac}(\ll 1)$ is the scalar elastic strain. The basic vibrational DOS $J(\varepsilon)$ can be calculated by applying its general formula [Eq. (6)] and the spectrum of eigenvalues of the vibrational excitations resulting from the equations of motion. As noted above in this section, in the original SMD model, the important distributions of values of the parameters for the soft-mode oscillators actually are reduced to the DOS $J_{sm}^{(0)}(\varepsilon')=g_{sm}^{(0)}(\nu')/2\nu'$.

The vibrational spectrum is found in a standard way from Eqs. (2) and (3) for well-defined wavelike vibrational excitations $\{x_{sm}(\mathbf{r},t),\mathbf{u}_{ac}(\mathbf{r},t)\}\propto\exp\{i(\mathbf{qr}-2\pi\nu t)\}$ with wave vectors $\mathbf{q}$ and small frequency half-widths $\gamma_{exc}\ll\nu_{exc}$. The spectrum is a polariton like two-branch one with the dispersion law $\varepsilon(q,\varepsilon')\equiv\nu_j^2(q,\varepsilon')$, $j=1,2$, at a given value of the bare soft-mode parameter $\varepsilon'\equiv\nu'^2$:

$$\varepsilon(q;\varepsilon')=\epsilon_j(q,\varepsilon')=\left(\tfrac{1}{2}\right)(\varepsilon'+s^2q^2/4\pi^2+\Delta)\{1+(-1)^j\times[1-\pi^{-2}\varepsilon's^2q^2(\varepsilon'+s^2q^2/4\pi^2+\Delta)^{-2}]^{1/2}\},\tag{4}$$

at $q\equiv|\mathbf{q}|=2\pi/\lambda_{ac}$. Here, $\Delta\simeq c_{sm}Q^2\varepsilon'$ and a typical Q^2, e.g., $Q^2=\beta^2(\mu_{av}s_0^2\mu_{sm}\nu_0^2a_0^2)^{-1}\approx 10$ for a typical soft-mode coupling parameter, $\beta^2\approx 1$ eV, and $\mu_{av}s_0^2\approx 10$ eV, $\mu_{sm}\nu_0^2a_0^2\sim 0.01$ eV, $a_0=1$ Å. The branches are separated by a narrow gap of a width Δ, $\Delta=\epsilon_{2,\min}-\epsilon_{1,\max}\approx 0.1\varepsilon_0$, at $\epsilon_{2,\min}=\varepsilon'\approx\varepsilon_0$, $\epsilon_{1,\max}=\varepsilon'(1-c_{sm}Q^2/\varepsilon_0)^{1/2}$, and $\varepsilon_0\equiv\nu_0^2$ [see Fig. 1 in Ref. 7(a)]. This is the most remarkable feature of the derived spectrum of excitations as hybridized acoustic and soft-mode vibrational ones. If the acoustic-soft-mode coupling parameter $\beta=0$, the gap disappears ($\Delta=0$) and two separate branches occur for noninteracting soft-mode vibrational excitations, $\nu=\nu'$, and acoustic phonons, $\nu\simeq s_0q/2\pi$. For frequencies relatively far from the gap, the dispersion relations $\nu_j^2(q,\varepsilon')$ of the well-defined excitations actually are similar to those of acoustic excitations with a sound velocity

$s \simeq s_0(1-\Delta\omega_0^{-2})^{1/2} \simeq s_0$: $\epsilon_1(q,\varepsilon') \simeq s_0^2 q^2/4\pi^2$ (standard sound waves) at $q < q_0 = 2\pi\nu_0/s_0$, while $\epsilon_2(q,\varepsilon') \approx \nu_0^2 + s^2q^2/4\pi^2$ at $q_0 < q < q_M = \nu_M/s_0$ ($\ll q_D = \nu_D/s_0$), both with a small frequency half-width due to the weak inelastic soft-mode-acoustic scattering $\gamma_{exc} < \nu_{ac} = s_0 q/2\pi$. In this connection, the upper branch is similar to the abovementioned HFS with an empirical upper limit frequency $\nu_M \approx (2-3)\nu_{BP}$.[3] For instance, for $sq < \nu_0$, γ_{exc} and the related acoustic mean-free path $l_{ac}^{(in)}$ are readily estimated in the general soft-mode model by applying the standard scattering theory and accounting for the basic bare soft-mode DOS $J_{sm}^{(0)}(\nu')$, $\gamma_{ac}^{(in)}(\nu) \approx \nu_0(\nu/\nu_0)^\alpha < \nu_0$, and, e.g., $l_{ac}^{(in)}(\nu') \approx \lambda_{ac}(\nu_0)(\nu_0/\nu')^{\alpha+1} > \lambda_{ac}(\nu_0)$ (e.g., see Ref. 22).

Another major feature of the resulting spectrum of hybridized acoustic and soft-mode vibrational excitations is the occurrence of quite different states of THz scale frequencies around the gap, which are not described by the equations of motion of Eq. (2). These states are not expected to be well-defined excitations because their widths are large [i.e., of the scale of the frequencies ("ill-defined excitations"); e.g., see Ref. 20], by the definition of the related Ioffe-Regel crossover. This can be seen from a scale estimation of $l_{ac}^{(in)}(\nu')$ and $\gamma_{ac}^{(in)}(\nu')$ for the states around the gap edges, by extrapolating the above estimations to $\nu' \approx \nu_0 \sim 1$ THz,

$$l_{ac}^{(in)}(\nu') \approx \lambda_{ac}(\nu') \quad \text{and} \quad \gamma_{ac}^{(in)}(\nu') \approx \nu' \quad \text{at } \nu' \approx \nu_{IR}^{(in)} \simeq \nu_0, \tag{5}$$

where $\nu_{IE}^{(in)}$ is the characteristic frequency $\nu_{IR}^{(in)}$ of the crossover from a weak-inelastic scattering and a weak hybridization of both types of the bare excitations in a well-defined wavelike excitation to a strong scattering and a strong hybridization of the bare excitations in an extended ill-defined excitation.

For calculations of the basic DOS $J(\varepsilon)$ from its general formula [see Eq. (6)], the standard approximation based on the δ function describing the excitations energy conservation and defined in Eq. (A1) can be applied only for the well-defined excitations relatively far from the gap edges. However, this approximation is not expected to hold for the ill-defined excitations, so that the δ function has to be replaced by an appropriate regular function in order to account for the large widths of the excitations (Sec. III). Then, both the calculated basic DOS $J(\varepsilon) = g(\nu)/2\nu$ and reduced frequency DOS $g(\nu)/\nu^2$ [see Ref. 7(b)] exhibited a pronounced broad peak of a similar asymmetric shape and a large half-width $\gamma_{IR}^{(in)} \simeq \nu_{IR}^{(in)} \simeq \nu_0$. This peak was identified as a BP in the scattering intensities [Eq. (15)] at $\nu \simeq \nu_{BP} \simeq \nu_{IR}^{(in)} \simeq \nu_0$ with a half-width $\gamma_{BP} \simeq \gamma_{IR}^{(in)}$. Above the BP, both $J(\varepsilon)$ and $g(\nu)/\nu^2$ exhibit a Debye-like behavior suggested to describe a HFS. The calculations were performed by using the abovementioned power-law basic DOS $J_{sm}^{(0)}(\varepsilon')$ for the soft-mode vibrations (at $\alpha = 1$).

III. COMPLETE SOFT-MODE-DYNAMICS MODEL OF VIBRATIONAL ANOMALIES: BASIC RELATIONSHIPS

Let us now present the basic relationships, obtained in the SMD model, which account also for the vibrational instability effect [Eq. (1)] and, in this sense, is the complete SMD model. The latter appears to considerably improve the analytical description of the BP and HFS and, in general, of the related vibrational anomalies in the glasses under consideration. The main idea of this SMD model is that the basic vibrational DOS $J^*(\nu'^2) = g^*(\nu')/2\nu'$, with $g^*(\nu')$ of Eq. (1) for the soft-mode vibrations renormalized by their elastic interactions, has to be substituted for the simplest basic soft-mode DOS $J_{sm}^{(0)}(\nu'^2)$ containing two parameters, ν_0 and α (Sec. II). The resulting SMD model has a clear advantage over the original SMD model: the soft-mode vibrational DOSs $J^*(\nu'^2)$ and $g^*(\nu')$ appear to contain a single material parameter related to the characteristic excitation frequency. The spectral characteristic calculated in the present model is the basic vibrational DOS $J(\varepsilon)$ for the spectrum of the vibration eigenvalues, $\varepsilon = \varepsilon(q) = \nu^2(q)$

$$J(\varepsilon) = \int_{\varepsilon_1'}^{\varepsilon_2'} d\varepsilon' J_{sm}(\varepsilon') I(\varepsilon;\varepsilon') = g(\nu)/2\nu, \tag{6}$$

where $J_{sm}(\varepsilon' \equiv \nu'^2)$ is the basic vibrational soft-mode DOS and $I(\varepsilon;\varepsilon')$ is the kernel transforming bare soft-mode vibrational excitations into resulting vibrational excitations due to acoustic-soft-mode interactions. Moreover, in Eq. (6), $\varepsilon_1' \simeq (3w/h)^2 \approx 0.1\nu_0^2$ is the lower limit of the integral, while $\varepsilon_2' \approx \nu_0^2$ ($\ll \nu_D^2$) is its upper limit (Sec. II). The basic soft-mode DOS is $J_{sm}(\varepsilon') = J_{sm}^{(0)}(\varepsilon')$ for independent soft-mode vibrational excitations, while $J_{sm}(\varepsilon') = J^*(\varepsilon' = \nu_r'^2)$ for those renormalized due to the elastic interactions. As well as in Sec. II, both $J(\varepsilon)$ and $J_{sm}(\varepsilon')$ are normalized to unity, e.g., $\int J(\varepsilon)d\varepsilon = \int g(\varepsilon^{1/2})d(\varepsilon^{1/2}) = 1 = \int g_{sm}^{(0)}(\nu')d\nu'$.

In what follows, we compare the qualitative behavior of the measurable basic DOS $J(\varepsilon)$ and reduced DOS $g(\nu)/\nu^2$ in both the complete and original SMD models for understanding the relative roles of the IRC for inelastic scattering and the vibrational instability effect. For calculations of the transformation kernel $I(\varepsilon;\varepsilon')$, the defining equations of the SMD model, Eqs. (2)–(6), are applied and account for the following basic statements of the SMD model.

(i) For a given soft-mode frequency ν', the spectrum of the wavelike excitations is determined by the basic equations of motion [Eqs. (2) and (3)] and consists of two branches [Eq. (4)] separated by a narrow gap of a typical width $\Delta \simeq \Delta_0 \approx 0.1\nu_0^2$. The upper branch above the gap at $\nu' \approx \nu_0$ corresponds to propagating acousticlike excitations with properties similar to those of the experimentally observed HFS.

(ii) The excitations around the gap are constructed of strongly hybridized acoustic and soft-mode vibrations around the IRC for the inelastic scattering of the vibrations [Eq. (5)]. In the IRC region [$\nu \approx \nu_{IR}^{(in)} \simeq \nu_0$, at $l_{ac}^{(in)}(\nu_{IR}^{(in)}) = \lambda_{ac}(\nu_{IR}^{(in)})$], the excitations are ill-defined states of large frequency width, $\gamma_{ac}^{(in)}(\nu_{IR}^{(in)}) \equiv \gamma_{IR}^{(in)} \simeq \nu_0$.

(iii) The consistent analytical theory for the vibrational states and their DOS around the IRC under discussion does not appear to be available at present, because standard perturbation-theoretical expansions of the scattering theory with a small parameter, $\vartheta \equiv \lambda_{ac}(\nu')/l_{ac}^{(in)}(\nu') \approx \gamma_{ac}^{(in)}(\nu')/\nu'$

$\ll 1$, fail around the IRC, at $\vartheta \approx 1$. In this sense, the defining relationship of the SMD model in the IRC region, and beyond it, is Eq. (6) for the basic DOS, for which the standard approximation $I(\varepsilon;\varepsilon') \simeq I_0(\varepsilon;\varepsilon')$ for the wavelike excitations is described in Eq. (A1). For numerical calculations, the δ function in $I_0(\varepsilon;\varepsilon')$ has to be approximated by a "prelimit" regular function $D[\varepsilon - \epsilon_j(q;\varepsilon'); \eta = \eta_1]$, and the result is weakly sensitive to a specific form of the function and to a specific value of the small parameter $\eta_1(\to +0)$. Since, however, the standard approximation and the perturbation-theoretical approach fail in the IRC region $\varepsilon \approx \nu_0^2$, a phenomenological ansatz in accordance with the definition of the IRC [Eq. (5)] is introduced for calculating the basic DOS $J(\varepsilon)$ at such ε. The ansatz is a Lorentzian-like function $D[\varepsilon - \epsilon_j(q;\varepsilon'); \eta = \eta_2]$ substituted for the δ function with a much larger parameter $\eta_2 \approx 1$ for the half-width $\gamma_{IR}^{(in)} \equiv \eta_2 \nu_0 \approx \nu_{IR}^{(in)} \simeq \nu_0$

$$D[\varepsilon - \epsilon_j(q;\varepsilon'); \eta_2] = \eta_2 \nu_0^2 / \pi[(\varepsilon - \epsilon_j(q;\varepsilon'))^2 + \eta_2^2 \nu_0^4]. \tag{7}$$

One can suggest from the definition of the IRC that the coherence of the acoustic phonon plane-wave phases is essentially violated in the related eigenstates approximated by superpositions of the waves and quasilocal vibrational soft-mode states with appropriate coefficients having rather irregular phases, which cannot be calculated explicitly in the absence of the consistent perturbation-theoretical approach. Since, by this definition, the IRC frequency is still lower than the "mobility" (localization) edge frequency, one can suggest for estimations that the eigenstate in the IRC region can be rather a nonlocalized one and characterized by a diffusive motion and an effective diffusion coefficient $D_{eff} \approx V_{eff}^2 \gamma_{eff}^{-1}$ (than a localized state with $V_{eff}=0$), but not a propagating wavelike state with the sound velocity s_0. Then, the group velocity V_{eff} is much smaller than s_0: $V_{eff} \approx (D_{eff}\gamma_{eff})^{1/2} \approx (a_1^2 \nu_{eff}\gamma_{eff})^{1/2} \lesssim a_1 \nu_{BP} \approx 3 \times 10^4$ cm/s $\approx 0.1 s_0$, where the effective frequency and width are, respectively, $\nu_{eff} \approx \nu_{BP} \approx 1$ THz and $\gamma_{eff} \approx \gamma_{IR}^{(in)} \approx \nu_{IR}^{(in)}$.

It is convenient in what follows to calculate dimensionless expressions describing $J(\varepsilon)$ and $g(\nu)/\nu^2$ by introducing dimensionless variables and parameters and choosing the typical frequency ν_0 as the scale

$$u \equiv \varepsilon/\nu_0^2 \equiv \nu^2/\nu_0^2, \quad t \equiv \varepsilon'/\nu_0^2, \quad \delta \equiv \Delta/\nu_0^2 \quad \text{and} \quad z \equiv \epsilon/\nu_0^2. \tag{8}$$

The expression for the dimensionless basic DOS follows from Eq. (A4) derived in the Appendix and can be presented as

$$\mathbf{J}(u) = \nu_0^2 J(\varepsilon) = C_{ac} \int_{\Omega(z,t)} dt \int dz \sqrt{z} \mathbf{J}_{sm}(t) g(z;t;\delta) \mathbf{D}(z-u;\eta) = \mathbf{g}(\sqrt{u})/2\sqrt{u}, \tag{9}$$

where $\mathbf{J}(u) = \mathbf{g}(u^{1/2})/2u^{1/2}$ and $\mathbf{J}_{sm}(t) \equiv \nu_0^2 J_{sm}(\kappa t)$; $\mathbf{J}_{sm}(t) \equiv \mathbf{J}_{sm}^{(0)}(t) = t^{(\alpha-1)/2}$ at $\alpha = 1;2;3;4$ or $\mathbf{J}_{sm}(t) \equiv \mathbf{J}^*(\kappa t) \approx (\kappa t)^{3/2} \int_0^1 dz [1 + (\kappa t)^3 z^2 (3 - 2z^2)]^{-1}$; $g(z,t;\delta) \equiv [(z-t-\delta)/(z-t)]^{1/2}[1 + t\delta/(z-t)^2]$. Moreover, $\mathbf{D}(z-u;\eta) \equiv \eta/\pi[(z-u)^2 + \eta^2]$ with $\eta = \eta_1 \ll 1$ (e.g., $\eta_1 \lesssim 10^{-2}$) for the wavelike excitations, whereas $\eta = \eta_2 \approx 1$ in the IRC region, and $C_{ac} = (3/2) u_D^{-3/2}$ at $u_D \equiv \nu_D^2 \nu_0^{-2}$. By definition, $\kappa \equiv 1$ for $\mathbf{J}_{sm} \equiv \mathbf{J}_{sm}^{(0)}$, while $\kappa \equiv (\nu_0/\nu^*)^2$ may be considered as the single parameter of the theory for $\mathbf{J}_{sm} \equiv \mathbf{J}^*$. The integration procedure in $\mathbf{J}(u)$, applied in Ref. 7 at $\mathbf{J}_{sm}(t) = \mathbf{J}_{sm}^{(0)}(t) = t^{(\alpha-1)/2}$ ($\alpha = 1$), is straightforwardly related to the integration in Eq. (A4) and extended not only to $\alpha = 2;3;4$, but also to the alternative renormalized bare DOS $\mathbf{J}_{sm}(t) = \mathbf{J}^*(\kappa t)$. The respective integration range $\Omega(z,t)$ for the double integral in Eq. (9) consists of four two-dimensional ranges described in Eqs. (A5) and (A6). It appears reasonable to perform the calculations for κ varying in the range $1 \lesssim \kappa \lesssim 10$, since plausibly one may suggest in the vibration-instability model that $(w/h \lesssim)\, \nu^* \lesssim 0.3 \nu_c \lesssim \nu_0$ at $\nu^* \ll \nu_c \ll \nu_D$. Then, one can readily obtain from Eqs. (9) and (A3)–(A6) that the dimensionless DOS $\mathbf{J}(u)$ can be expressed as a sum of two double integrals,

$$\mathbf{J}(u) = \mathbf{g}(\sqrt{u})/2\sqrt{u} = [\mathbf{F}(u) + \mathbf{G}(u)], \tag{10}$$

$$\mathbf{F}(u) = \int_{t_1}^{t_2} dt \mathbf{J}_{sm}(t) \left[\int_{z_{\min}}^{t_1 - \varsigma} dz \sqrt{z} \mathbf{D}(z-u;\eta_1) g(z,t;\delta) + \int_{t_2+\delta}^{z_{\max}} dz \sqrt{z} \mathbf{D}(z-u;\eta_1) g(z,t;\delta) \right], \tag{11}$$

at $\eta_1 \ll 1$, and

$$\mathbf{G}(u) = \int_{t_1 - \varsigma}^{t_2 - \varsigma} dz \sqrt{z} \mathbf{D}(z-u;\eta_2) \int_{z+\varsigma}^{t_2} dt \mathbf{J}_{sm}(t) g(z,t;\delta) + \int_{t_1+\delta}^{t_2+\delta} dz \sqrt{z} \mathbf{D}(z-u;\eta_2) \int_{t_1}^{z-\delta} dt \mathbf{J}_{sm}(t) g(z,t;\delta), \tag{12}$$

at $\eta_2 \approx 1$, where $\sqrt{u} \equiv \nu/\nu_0$

Besides the typical value of the soft-mode vibration frequency $\nu_0 \approx 1$ THz and the characteristic frequency ν^* in Eq. (1), the parameters of the basic equations and results in the theory [Eqs. (2)–(12)], are as follows:

$$\nu_{IR}^{(in)} \simeq \nu_0, \quad \gamma_{IR}^{(in)} \simeq \nu_0,$$

$$t_i = \varepsilon_i' \nu_0^{-2}, \quad i = 1,2,$$

$$z_{\min} = \epsilon_{\min} \nu_0^{-2}, \quad z_{\max} = \epsilon_{\max} \nu_0^{-2}, \quad \varsigma = |z-t|_{\min} > 0, \quad \delta = \nu_0^{-2} \Delta, \tag{13}$$

where $\nu_{IR}^{(in)}$ is the IRC frequency (i.e., the boson-peak one) and $\gamma_{IR}^{(in)}$ is the peak half-width; $\varepsilon_{1,2}'$ or $\epsilon_{\min,\max}$ are the lower or upper limit for the respective integrals in Eqs. (10)–(12); Δ is the gap width and ς is the lower value of $|t-z|$ for cutting off the divergence of the integral in Eq. (12) at $|t-z| \to 0$ (see also Appendix).

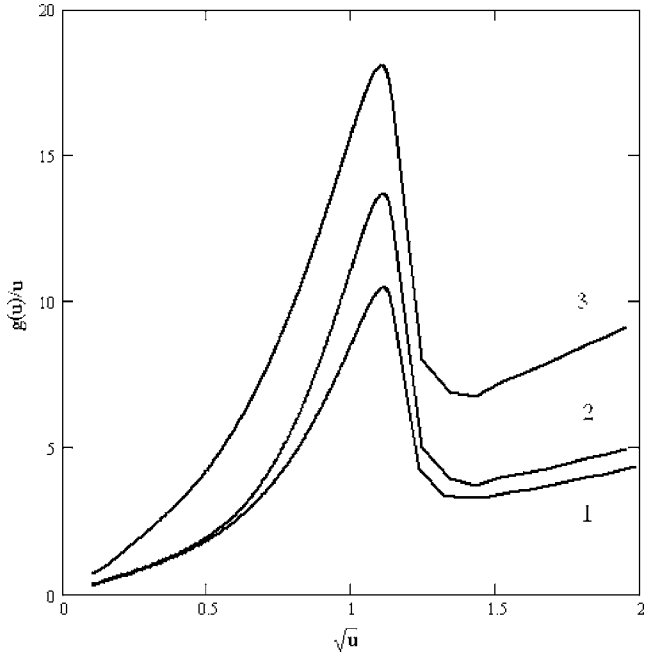

FIG. 1. The dimensionless reduced DOS described by $\mathbf{g}_r(u^{1/2})$ (in a.u.) as a function of $u^{1/2} \equiv \nu\nu_0^{-1}$. Here $\mathbf{J}_{sm}(t) = t^{(\alpha-1)/2}$ at $\alpha=2$ (curve 1), and $\mathbf{J}_{sm}(t) \equiv \mathbf{J}^*(\kappa t)$ at $\kappa=1$ (curve 2) and $\kappa=10$ (curve 3); values of the main parameters are defined in Eq. (18).

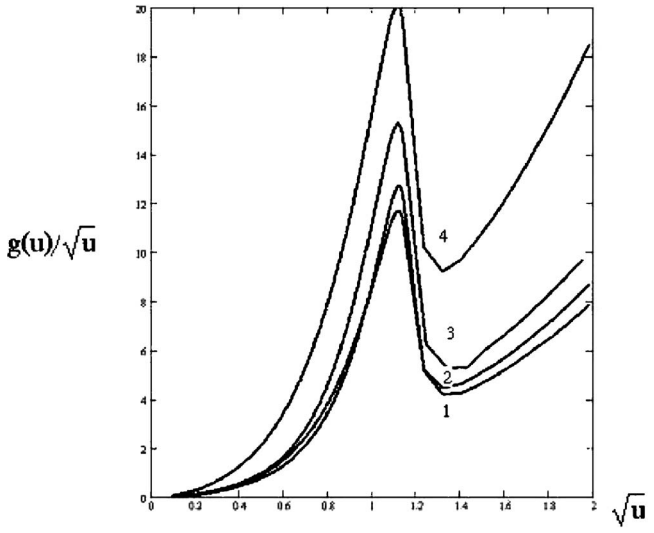

FIG. 2. The dimensionless doubled basic vibrational DOS described by $2\mathbf{J}(u)$ (in a.u.) as a function of $u^{1/2} \equiv \nu\nu_0^{-1}$, normalized to unity. Here $\mathbf{J}_{sm}(t) \equiv \mathbf{J}^*(\kappa t)$ at $\kappa=1$ (curve 1) and $\kappa=10$ (curve 2), and $\mathbf{J}_{sm}(t) = t^{(\alpha-1)/2}$ at $\alpha=2$ (curve 3) and $\alpha=3$ (curve 4); values of the main parameters are given in Eq. (18).

IV. ANOMALOUS PROPERTIES: DISCUSSION OF RESULTS AND COMPARISON WITH EXPERIMENT AND OTHER MODELS

In accordance with the purpose of the present article (Sec. I), the following principal question has to be answered: Is the IRC for the inelastic scattering of acoustic and soft-mode vibrations the most important phenomenon, or is the renormalization of the soft-mode vibrations by their elastic interactions equally important, for determining the qualitative properties of the dynamic vibrational anomalies, including the BP position (ν_{BP}) and the scale of its width ($2\gamma_{BP}$). The answer can be found from the results of numerical calculations of the dimensionless reduced DOS $\mathbf{g}_r(u^{1/2}) \equiv \mathbf{g}(u^{1/2})/u$ and basic vibrational DOS $\mathbf{J}(u) \equiv \mathbf{g}(u^{1/2})/2u^{1/2}$ as functions of $u^{1/2} \equiv \nu/\nu_0$, which are carried out from Eqs. (10)–(12) and the MATHCAD program—OMIT. Both the original soft-mode DOS, $J_{sm}(t) \equiv J_{sm}^{(0)}(t) = t^{(\alpha-1)/2}$ at $\alpha=2$ and 3, and the renormalized soft-mode DOS [Eq. (1)], $\mathbf{J}_{sm}(t) \equiv J^*(\kappa t)$ at $\kappa=1$ and 10 normalized to unity, are applied in the calculations, e.g., $\int \mathbf{J}(u)du = \int \mathbf{g}(u^{1/2})d(u^{1/2}) = 1 = \int g_{sm}(\nu')d\nu'$. The following characteristic values of the "free" parameters are mainly applied [see Eq. (13) and Appendix]:

$$t_1 = 0.1, \quad t_2 = 1,$$

$$z_{\min} = 0, \quad z_{\max} = 6,$$

$$\eta_1 = 10^{-2}, \quad \eta_2 = 1,$$

$$\varsigma = 0.05,$$

$$\delta = 0.1. \tag{14}$$

The results for $\mathbf{g}_r(u^{1/2})$ as a function of $u^{1/2} = \nu/\nu_0$ are presented in Fig. 1 with $\mathbf{J}_{sm}(t)$ at $\kappa=1$ and 10 as well as at $\alpha=2$, and show a broad asymmetric peak that, by the usual definition, is a boson peak in the reduced scattering intensity $I_R^{(r)}(\nu)$ [Eq. (15)] at $u^{1/2} \simeq 1$, i.e., $\nu/\nu_0 \simeq 1$. A weak increase of $\mathbf{g}_r(u^{1/2}) \propto \nu^\theta$ with increasing ν at $0 \lesssim \theta < 1$ (cf. the Debye behavior at $\theta=0$) is also available above the peak in Fig. 1. One can see from the figure that the qualitative features, including the peak position, of $\mathbf{g}_r(u^{1/2})$ are weakly sensitive to the difference in the soft-mode DOS itself, $\mathbf{J}_{sm}(t) = t^{(\alpha-1)/2}$ at different α or $\mathbf{J}_{sm}(t) = \mathbf{J}^*(\kappa t)$ at different κ. The behavior of $g_r(u^{1/2})$ above the BP is similar to, though relatively weakly deviates from, the Debye behavior. The similarity may be interpreted as a manifestation of the existence of the high-frequency acousticlike excitations in the upper spectral branch ($j=2$) of Eq. (4), similar to the experimentally observed HFS one. The origin of the deviation is not yet quantitatively understood, though it can be assumed as partly at least due to an appropriate weak dispersion of the HFS velocity $s_2(q) \simeq 2\pi\nu_2(q)/s_0$ at $q_0 = 2\pi\nu_0/s_0 < q < q_M$.

The results for the basic vibrational DOS $\mathbf{J}(u)$ vs $u^{1/2} \equiv \nu/\nu_0$ are shown in Fig. 2 at different $\alpha=2$ and 3 (qualitatively similar to the result in Ref. 7 at $\alpha=1$) and also $\kappa=1$ and 10, as well as in Fig. 3 at $\kappa=1$ and different values of the gap width, $\delta=0.05; 0.10; 0.15$ [i.e., of the soft-mode-acoustic coupling parameter β in Eq. (3)] around the typical $\delta=0.10$. As seen from Figs. 2 and 3, $\mathbf{J}(u)$ also exhibits a broad peak of an asymmetric shape and a large half-width $\gamma_{IR}^{(in)} \simeq \nu_{IR}^{(in)} \simeq \nu_0$, which is qualitatively quite similar to the boson peak in the reduced DOS and, thus, may be identified as the BP in the scattering intensity related to the Raman dynamic susceptibility χ_R'' [Eqs. (15)] at practically the same position $\nu = \nu_{BP} \simeq \nu_{IR}^{(in)} \simeq \nu_0$. Above the peak, $\mathbf{J}(u)$ exhibits a Debye-like increase with increasing ν, $\mathbf{J}(u) \propto \nu^{1+\theta}$, which similarly can be considered as characteristic of the experimentally ob-

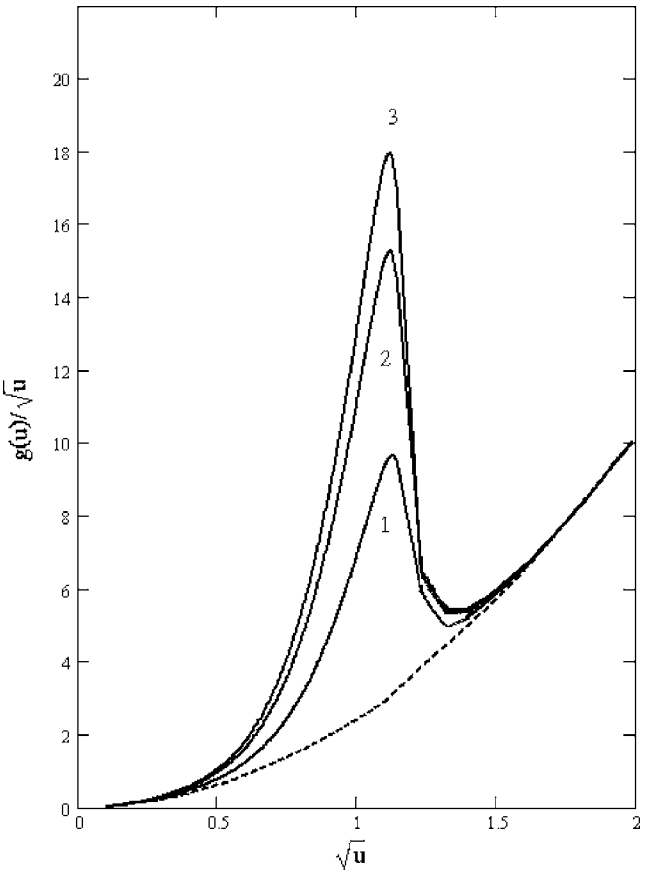

FIG. 3. The dimensionless doubled basic vibrational DOS described by $2\mathbf{J}(u)$ (in a.u.) as a function of $\delta \equiv \Delta/\nu_0^2 \propto \beta^2$, at $\mathbf{J}_{sm}(t) \equiv \mathbf{J}^*(\kappa t)$ at $\kappa=1$. Curve 1 is obtained at $\delta=0.05$ [$\beta^2=0.5$ (eV)^2], curve 2 at $\delta=0.1$ [$\beta^2=1$ (eV)^2] and curve 3 at $\delta=0.15$. The dashed curve is given for the hypothetical case at $\beta=0=\delta=\varsigma$. The values of main parameters are presented in Eq. (18); typical values of the parameters for the gap width are: $c_{sm}=5\times10^{-2}$, $\mu_{sm}=5\mu_{av}$, $\mu_{av}=10^{-22}$ g, $\nu_0=10^{12}/s$, $s_0^2=10^{11}$ (cm/s)^2.

served HFS. The qualitative features, including the peak position, of $\mathbf{J}(u)$ are also weakly sensitive to the difference in the soft-mode DOS itself, i.e., to the specific values of α or κ (at the typical value of $\delta=0.1$) in Fig. 2, as well as to specific values of δ at the given $\kappa=1$ in Fig. 3. For the hypothetical case at $\beta=0=\delta$ [see below Eq. (4)], the gap disappears between the two separate branches for noninteracting acoustic phonons ($\nu \simeq s_0 q/2\pi$) and soft-mode excitations ($\nu=\nu'$), and the IRC does not occur. Then, in Eqs. (9)–(12), the function $g(z,t;\delta=0)=1$ and $D(z-u;\eta)$ is a δ function, $D(z-u;\eta)=\delta(z-u)$, at both $\eta=\eta_1\to+0$ and $\eta=\eta_2\to+0$, and the integration ranges reduce to $t_1\leqslant t$, $z\leqslant t_2$ and $z_{\min}\leqslant z\leqslant z_{\max}$ at $\varsigma=0$ (see Appendix). The resulting basic DOS $J(u)$ becomes a product of the normalization integral for the soft-mode DOS (which is unity, by definition) and the Debye DOS $J_D(u)$ for the gapless acoustic spectrum, so that eventually $J(u)=J_D(u)$. This just follows from the calculations and is shown in Fig. 3 for comparison with the other three curves.

The results discussed above allow one to answer the principal question noted above Eq. (14) as follows. The IRC for the inelastic scattering of acoustic and soft-mode vibrations is here the most important phenomenon for determining the qualitative properties and thus the general origin of the dynamic vibrational anomalies, including the width scale and the frequency of the BP. At the same time, the renormalization of the soft-mode vibrations by their elastic interactions appears to be an effect contributing to quantitative characteristics like the values of the BP height and width. In fact, one can see in the figures considerable quantitative changes in the properties of the BP in Figs. 1 and 2 for different soft-mode DOSs at $\alpha=2$ and $\alpha=3$, with the strong hybridization of acoustic and soft-mode vibrational states only important, and at $\kappa=1$ and $\kappa=10$, with both the strong hybridization and the vibrational instability effect contributing to the BP, as well as at different values of δ in Fig. 3. On the other hand, in the HFS-like part of the curves, considerable quantitative changes are seen in Figs. 1 and 2 at different α or κ but not in Fig. 3 in which the curves are hardly distinguishable at different values of the gap width δ. The difference between the dependencies of the properties on α and κ and of those on δ appears to be due to the fact that the gap states [Eq. (9)] are essentially linked with the IRC (i.e., the BP), whereas no relation between the gap states and the HFS-like excitations and, thus, no substantial dependence of the HFS-like part of the curves on δ are available.

Let us now compare the results of the complete SMD model of the basic vibrational DOS $\mathbf{J}(u)$ and the reduced DOS $\mathbf{g}_r(u) \equiv \mathbf{g}(u^{1/2})/u$ with experimental data for the BP and associated effects in scattering intensities which in neutron scattering are usually described in terms of a peak of the reduced density of states, $g(\nu)\nu^{-2}$, of harmonic vibrational excitations, as the coupling coefficient of neutrons with the vibrations does not appear to depend on ν. The latter does not hold for the Raman coupling coefficient $c_R(\nu)$ of light with the vibrations, which may have diverse dependencies on ν for various groups of glasses. Then, generally speaking, the BP in the Raman scattering cannot necessarily be described as a peak of only the reduced density of states. Therefore, we concentrate on the Raman scattering data, of which comparison with different theoretical models seems to be most helpful for finding the relevant models of vibrational dynamics in glasses. In numerous Raman scattering experiments, the total scattering intensity $I_R(\nu,T)$, as well as the reduced intensity $I_R^{(r)}(\nu)$ and Raman dynamic susceptibility $\chi_R''(\nu)$ (by definition, both independent of T), are measured particularly for ν around the BP frequency ν_{BP}. The well-known phenomenological relationships for $I_R(\nu,T)$, $I_R^{(r)}(\nu)$, and $\chi_R''(\nu)$ are as follows:[23]

$$\begin{aligned} I_R(\nu,T) &= c_R(\nu)g(\nu)[1+n(\nu,T)]/\nu \\ &\equiv \chi_R''(\nu)[1+n(\nu,T)] \\ &\equiv I_R^{(r)}(\nu)\nu[1+n(\nu,T)], \end{aligned} \tag{15}$$

$$I_R(\nu,T) \propto c_R(\nu)g(\nu)\nu^{-\beta}. \tag{16}$$

Here $n(\nu,T)=[\exp(h\nu/k_BT)-1]^{-1}$ is a boson factor for effective scatterers, which are in this connection generally assumed to be extended harmonic vibrational excitations of THz frequency scale: $\beta\simeq2$ for high $T>h\nu_{BP}/k_B\equiv T_{BP}$ or

$\beta \simeq 1$ for low $T \lesssim T_{BP}$. According to a recent analysis of $c_R(\nu)$ from scattering intensity data for different glasses in the range between 10 and 50 cm^{-1} around the BP, two groups of glasses can be distinguished.[24] For the first group (e.g., SiO_2, B_2O_3, CKN, PC),

$$c_R(\nu) \propto [(\nu/\nu_{BP}) + B] \quad \text{at } B \approx 0.5, \tag{17}$$

with its high-frequency limit varying from about 2 ν_{BP} for SiO_2 and Se glasses up to about 4 ν_{BP} for PC glass. However, for the second group (e.g., As_2S_3, $GeSe_2$, GeO_2),

$$c_R(\nu) \propto \nu \quad \text{with } B \approx 0. \tag{18}$$

It is worth concluding that the BP in $I_R(\nu,T)$ at high T is the same as the one in $I_R^{(r)}(\nu)$, i.e., in the reduced DOS $g(\nu)\nu^{-2}$, for the first group of glasses with $c(\nu) \approx const$, or in $g(\nu)\nu^{-1}$, for the second group with $c_2(\nu) \propto \nu$. On the other hand, the BP in $I_R(\nu,T)$ at low T is the same as the one in $\chi_R''(\nu)$, i.e, the one in $g(\nu)\nu^{-1}$ for the first group of glasses or in $g(\nu)$ for the second group. In addition to numerous BP experimental data in scattering spectra of $I_R^{(r)}(\nu)$ [e.g., see Refs. 1 and 25 and references therein], the BP appears also to be observed in the spectra of $\chi_R''(\nu)$, in a number of different glasses like diglycidyl bisphenol A (DGEBA), polymethyl methacrylate (PMMA) (Ref. 26) and calcium potassium nitrate (CKN), polysterene, polycarbonate,[27] also with the characteristic frequency $\nu_{BP} \sim 1$ THz. Actually, the BP is observed in glasses not only in numerous experimental data for the reduced scattering intensity (e.g., see Refs. 1 and 25 and references therein), but also in data for the Raman dynamic susceptibility $\chi_R''(\nu)$ [Eq. (15)] in a number of glasses like DGEBA, PMMA (Ref. 26) and CKN, polysterene, polycarbonate.[27] In the present model, all the scattering intensities, including $\chi_R''(\nu)$ and the total scattering intensity, exhibit the broad asymmetric boson peak at $\nu = \nu_{BP} \simeq \nu_0 \sim 1$ THz and, above it, the "wing" corresponding to the HFS-like excitations characterized by a group velocity $s \simeq s_0$. In this sense, the model gives a rather complete qualitative (and probably scalewise) description of the correlated BP and HFS in the scattering spectra of the glasses under discussion, in qualitative accordance with the experimental data.

Unlike the SMD model, the vibration instability effect even in the reduced intensity of light gives rise to the BP only for one group of glasses [Eq. (17)], while not for another group [Eq. (18)], and does not lead to the observed HFS-like excitations. Moreover, one can conclude from this comparison that in the model with Eq. (1), the BP does not occur in the basic vibrational DOS $J(u)$ and, thus, in $\chi_R''(\nu)$ for both groups of glasses. Then, it follows from Eqs. (15)–(18) for Raman scattering intensities that a pronounced BP occurs in this model only in the reduced DOS; and, thus, in the reduced Raman scattering intensity $I_R^{(r)}(\nu) \propto g^*(\nu)\nu^{-1}[1+B(\nu_{BP}/\nu)]$ for the group of glasses with $B \approx 0.5$, while it does not for the other group with $B \approx 0$. However, all these conclusions are not in accordance with the referred-to experimental data.[26,27] In addition, the model with Eq. (1) does not give rise to the pronounced high-frequency sound wing observed above the BP in the glasses,[3] rather due to the neglect of the direct contributions of acoustic excitations and their interactions with the soft-mode vibrations accounted for in the SMD model. It is argued also in (Ref. 24) that the observed universality of the frequency dependence of the coupling coefficient in the Raman scattering intensity, for each of the two groups of glasses, supports the idea that the extended vibrational excitations cannot be separated into propagating and nonpropagating ones in the BP region. This idea seems to be in accordance also with the conclusion of the complete SMD model that a strong hybridization of propagating (acoustic) and nonpropagating (soft-mode) excitations occurs in the IRC determining the BP.

Experimentally observed thermal anomalies of glasses,[1,28] the "bump" of reduced specific heat at a characteristic $T = T_{\max} \simeq T_{BP} \equiv h\nu_{BP}/k_B \sim 50$ K, as well as the "plateau" at $T \approx T_{\max}$ and quasilinear increase at $T_{\max} \lesssim T < T_M \equiv h\nu_M/k_B \lesssim 100-150$ K of thermal conductivity, with increasing T can also be described by applying the SMD model to the general formulae for both quantities[1] in terms of the frequency DOS $g(\nu)$. The results of such a procedure have recently been presented, with an account for an earlier theory (see (Ref. 9) and references therein), by applying the original SMD model. The basic results of the complete SMD model practically remain the same for two reasons: (i) the shape of the bump is in a rather trivial way determined by thermal excitations ($h\nu \simeq k_B T \approx k_B T_{\max}$) in the IRC or BP region and, thus, is similar to the shape of the BP for the reduced DOS. (ii) Propagating HFS thermal excitations are assumed to be the heat carriers determining the major term, $\chi_0(T)$, of the thermal conductivity for the Boltzmann heat transport; however, in the BP region thermal excitations are expected to give rise to only a small correction $\Delta\chi(T) \neq 0$ for nonlocalized excitations. The assumption of a small finite correction for nonlocalized BP excitations can be justified by taking into account the estimations $V_{eff} \lesssim 0.1 s_0$ (Sec. III), $\gamma_{BP}/\gamma_{ac}(\nu_{BP}) \gtrsim 10$, and $g(\nu_{BP})/g_{ac}(\nu_{BP}) \lesssim 10$: $\Delta\chi(T_{BP})\chi_0^{-1}(T_{BP}) \approx (V_{eff}/s_0)^2[g(\nu_{BP})/g_{ac}(\nu_{BP})] \times [\gamma_{ac}(\nu_{BP})/\gamma_{BP}] \lesssim 10^{-2}$.

V. CONCLUSIONS

In the present complete SMD model, the origins of the correlated boson peak at $\nu \approx \nu_{BP}$, of a large half-width $\gamma_{BP} \approx \nu_{BP}$, and a high-frequency sound at $\nu > \nu_{BP}$ are determined by the Ioffe-Regel crossover from a weak inelastic scattering of acoustic phonons by vibrational excitations of (interacting) soft-modes to a strong scattering and a resulting strong hybridization of both types of excitations around a characteristic crossover frequency, identified as the BP frequency, the $\nu_{IR}^{(in)} \simeq \nu_{BP}$. The vibrational instability effect[13] (Sec. II) due to elastic interactions between the soft-mode vibrational excitations can change quantitative aspects of the original SMD model, but hardly its qualitative properties. Therefore, in the soft-mode related models, the strong hybridization of phonons with soft-mode vibrational excitations in the Ioffe-Regel crossover for inelastic scattering appears to be the major phenomenon determining the origin of dynamic and thermal anomalies in the glasses under consideration.

A comparison of the analytical SMD model with two other recent models, containing both analytical approaches[5,6] and simulations,[8,4] appears to show qualitative similarities between the SMD and the other models, although specific relations between the models still have to be investigated. The harmonic vibrational soft-mode excitations, renormalized by the vibrational instability effect and considered as the new bare excitations with a peak in their DOS, appear to play a role similar to that of the "anomalous-oscillation" excitations related to a BP in the vibrational DOS of the mode-coupling model.[5] The interactions and hybridization of the nonacoustic excitations, either with acoustic phonons in the SMD model or with "mesoscopic wavelength" density fluctuations in the mode-coupling model, turn out to produce similar high-frequency sound excitations in the glasses under discussion. In the Euclidean random matrices approach,[8] the basic result is a relevant analytical description of the high-frequency sound with qualitative properties similar to those in the present SMD model and in the mode-coupling model. The origin of the BP as an unavoidable dynamic property of glasses is analyzed in another mean-field model[4] and is related to the occurrence of a band for acoustic phonons and another band for excitations, "glassons," that also are rather of nonacoustic nature, and to the hybridization of both types of states with each other. At low temperatures, the glasson band is found to develop a gap which appears to show up as the BP in the reduced DOS $g(\nu)\nu^{-2}$. In this connection, it seems that there is also a qualitative similarity between the properties of glasson-phonon systems and those of soft-mode-phonon systems noted in the statements (i)–(iii) of Sec. III. Thus, each of these different mean-field models, giving rise to both a BP and a HFS, may play at present its role in understanding the phenomena. The advancements of the present SMD model seem to be as follows. (i) The nonacoustic excitations, interacting with the acoustic ones, are explicitly identified as the soft-mode vibrational excitations described in detail in the general soft-mode model (Sec. II) and are strongly correlated with the nonvibrational tunneling excitations that are also soft-mode excitations but of very low energies. This correlation agrees with the empirical fact that disordered materials, in which no glassy dynamic anomalies at very low temperatures are observed, do not exhibit a BP (Sec. II).

(ii) The SMD model gives a simple analytical description of the vibrational dynamic anomalies and can hint that intrinsically linear theories like Ref. 8 and nonlinear ones like the anharmonic soft-mode model may be in some aspects equivalent, at least in a mean-field approximation.

(iii) A simple extension of the SMD model describes thermal anomalies (the plateau and quasilinear increase of thermal conductivity with increasing temperature, etc.) of the glasses at moderately low temperatures.

The SMD model can also be compared to recent alternative models of the boson peak, accounting for only elastic scattering of phonons, mainly of acoustic ones, in a random static field of a disordered system.[14] In particular, in the models by Taraskin and Elliott, a "phase diagram" disorder vs frequency for the vibrational excitations in the system (e.g., a fcc lattice with force-constant disorder) has been derived, by using the analytical coherent-potential approximation and numerical solutions of the resulting equations. For most degrees of disorder, the boson peak in such systems is found to occur actually at the same frequency as the Ioffe-Regel crossover between weak and strong elastic scattering of the propagating vibrational excitations from the static disorder at the characteristic frequency $\nu_{IR}^{(el)} \simeq \nu_{BP}$. However, unlike the situation in systems with the Ioffe-Regel crossover for inelastic scattering, the high-frequency sound excitations do not seem to appear above the boson peak in these models.

As noted in earlier works, there is an essential difference between elastic and inelastic scattering and between the related Ioffe-Regel crossovers. Elastic scattering does not change the phase of the system wave function, and, thus, appropriate interference effects are anticipated to give rise to the Anderson localization above the "mobility edge" for acoustic phonons. The Ioffe-Regel crossover at a frequency lower than the edge generally precedes the localization of the excitations (e.g., see Ref. 20). On the other hand, taking into account the Heisenberg uncertainty for energy and phase fluctuations,[29] one can suggest that inelastic scattering changes the phase and does not necessarily give rise to the localization. In this sense, the inelastic scattering appears to favor extended excitation states. In fact, the Ioffe-Regel crossover under discussion can be characterized by eigenstates approximated by superpositions of acoustic waves and quasilocal soft-mode states with coefficients having rather irregular phases (Sec. IV). Then, the coherence of the wave phases is violated and the "localizing" interference effects related to the hybridized acoustic and soft-mode excitations can become weak. Thus the eigenstates in the crossover region, rather, are extended states, propagating waves outside the boson-peak region or nonpropagating states inside it. In this connection, the Ioffe-Regel crossover for inelastic scattering can produce propagating waves, like a high-frequency sound, even above the boson peak. Moreover, glasses with both a boson peak and a high-frequency sound seem to be adequately described in the models[5,7,8] accounting for both acoustic phonons and some nonacoustic excitations interacting with each other, rather than in models[14] accounting probably for only the phonons and the boson peak. The difference between glasses of both types can be ascribed to the distinction in the properties of inelastic and elastic scattering of (acoustic) phonons.

From this viewpoint, a universal feature of the boson peak is believed to be determined by the occurrence of Ioffe-Regel crossovers (and, probably, the nonlocalized type of the excitation states, which at present appears to be established at least in the models by Taraskin and Elliott,[14] accounting for the crossover for elastic scattering of acoustic phonons). A nonuniversal feature is suggested to be related to the occurrence of two distinct limit types of the dynamic anomalies and, in this sense, of glasses: (I) the glasses under discussion, for which two spectral branches of excitations separated by a gap are essential and the Ioffe-Regel crossover for inelastic scattering of the excitations can determine both the boson peak and high-frequency sound in the inelastic scattering spectra; (II) glasses for which (acoustic) phonons are most important, so that the Ioffe-Regel crossover for their elastic scattering can determine the boson peak. The suggestion of the two limit types of glasses seems to be consistent with

recent data for v-SiO_2 as a glass of type I (Refs. 3 and 30) and v-B_2O_3 as a glass of type II (Ref. 30). The criterion for the existence of glasses and vibrational anomalies of type I appears to be the inequality

$$\nu_{BP} \simeq \nu_{IR}^{(in)} \simeq \nu_0 < \nu_{IR}^{(el)} (\ll \nu_D), \tag{19}$$

while the inequality

$$\nu_{BP} \simeq \nu_{IR}^{(el)} < \nu_{IR}^{(in)} (\ll \nu_D) \tag{20}$$

is the criterion for the existence of glasses and vibrational anomalies of type II.

For a glass of type I, the propagating high-frequency sound excitations are expected to occur for not too high ν, $\nu_{BP} < \nu < \nu_M \equiv p_{\max}\nu_0$, with the crossover frequency $\nu_{IR}^{(el)} \equiv \nu_M$ for the high-frequency sound excitations elastically scattered [$p_{\max}$ can be here identified with the experimental value $p_{\max}^{(\exp)} \approx 2-3$ (Ref. 3)]. The hybridization of the bare soft-mode vibrational excitations with the phonons appears to extend the SMD theory to higher ν, $\nu_0 < \nu < \nu_M$, than those of the bare soft-mode excitations. Moreover, a finite frequency range $\nu_M < \nu < \nu_{loc}$ is expected to occur, in which the excitations are still extended but in nonpropagating states; ν_{loc} denotes the mobility edge for acoustic phonons. In this connection, a corresponding range of higher temperatures T, $T_M < T < T_{loc} \equiv h\nu_{loc}/k_B$ with $T_M \approx 100-150$ K, may exist, in which another (probably less pronounced) plateaulike behavior could be observed in the thermal conductivity. So far it is difficult to present specific estimations of the frequencies $\nu_{IR}^{(in)}$ ($\simeq \nu_0$) and $\nu_{IR}^{(el)}$ in terms of measurable properties; thus, the type of a glass cannot be established independently of inelastic scattering experiments.

ACKNOWLEDGMENT

We are grateful to our colleague Vivian Halpern for reading the manuscript and for useful remarks.

APPENDIX

In this appendix, the analytical expression for the basic vibrational DOS $J(\varepsilon)$, describing the spectrum of the vibration eigenvalues $\varepsilon = \varepsilon(q) = \nu^2(q)$ with the dispersion law $\nu(q)$ of the spectrum, is derived by using Eqs. (10)–(12) and the procedure developed in Ref. 7 for the case of a bare DOS $J_{sm}(\varepsilon' \equiv \nu'^2) = J_{sm}^{(0)}(\varepsilon') \approx \nu_0^{-2}(\varepsilon'/\nu_0^2)^{(\alpha-1)/2}$ at $\alpha = 1$ (Sec. II) and also at $\alpha = 2;3;4$ (Sec. IV) and by extending it to other cases with the bare DOS $J_{sm}(\varepsilon') = J^*(\varepsilon')$ (Sec. IV). The standard approximation of the transformation kernel $I(\varepsilon;\varepsilon')$ in Eq. (6) for well-defined sound-wave-like excitations below and above the IRC region, at a given $\varepsilon' \equiv \{\nu'^2 \text{ or } \nu_r'^2\}$, is as follows:

$$I(\varepsilon;\varepsilon') \simeq I_0(\varepsilon;\varepsilon') = \left(\frac{2\pi}{a_1}\right)^3 \Sigma_{j=1,2} \int (d\mathbf{q})\, \boldsymbol{\delta}[\varepsilon - \epsilon_j(q;\varepsilon')]. \tag{A1}$$

It is taken into account that the spectrum of for the excitations [Eq. (3)] consists of two branches ($j = 1,2$) separated by a narrow gap. As usual for numerical calculations, the function $\delta[\varepsilon - \epsilon_j(q;\varepsilon')]$ can be here replaced by its prelimit regular approximation $D(Y)$

$$\delta(Y) = \lim_{\eta \to +0} \eta\nu_0^2 \pi (Y^2 + \eta^2 \nu_0^4) \simeq D(Y) = \eta_1 \nu_0^2 \pi (Y^2 + \eta_1^2 \nu_0^4) \equiv D(Y;\eta_1), \tag{A2}$$

the result being weakly sensitive to specific expression of $D(Y)$ and value of $\eta = \eta_1 \approx \gamma_j(q)\nu_0^{-1} \ll 0.1$, e.g., $\eta_1 \lesssim 0.01$, with $\gamma_j(q)$ the half-width of the eigenfrequency $\nu_j(q)$. For calculating the basic vibrational DOS in the IRC region, its expression can readily be derived with the phenomenological ansatz of Eq. (7) in which a much larger parameter $\eta = \eta_2 \approx 1$ is substituted for the parameter η. Then, the basic vibrational DOS can be expressed as follows:

$$J(\varepsilon) = (a_1/2\pi)^3 \Sigma_{j=1,2} \int_{\Omega(\mathbf{q})} (d\mathbf{q}) \times \int_{\varepsilon_1'}^{\varepsilon_2'} d\varepsilon' J_{sm}(\varepsilon') D[\varepsilon - \epsilon_j(q;\varepsilon');\eta], \tag{A3}$$

where $\Omega(\mathbf{q})$ is the range of the allowed wave-vector values. The integration procedure in Eq. (A3) developed in (Ref. 7) took into account that the dispersion relationship [Eq. (3)] is independent of the $\mathbf{q}$ direction. Then one readily gets that

$$J(\varepsilon) = 4\pi(a_1/2\pi)^3 \Sigma_{j=1,2} \int_{\varepsilon_1'}^{\varepsilon_2'} d\varepsilon' J_{sm}(\varepsilon') \times D[\varepsilon - \epsilon_j(q;\varepsilon');\eta] \int_{\Omega(\epsilon_j,\varepsilon')} Q(\epsilon;\varepsilon') d\epsilon, \tag{A4}$$

where $Q(\epsilon;\varepsilon') = q^2(\epsilon;\varepsilon')(\partial q(\epsilon,\varepsilon')/\partial\epsilon) = (1/2s^3)[\epsilon(\epsilon-\varepsilon'-\Delta)/(\epsilon-\varepsilon')]^{1/2} \times [1 + \varepsilon\Delta/(\epsilon-\varepsilon')^2]$ and $q(\epsilon;\varepsilon')$ is the appropriate solution of the equation $\epsilon(q;\varepsilon') = \epsilon$, while $\Omega(\epsilon,\varepsilon')$ denotes the variation range including such ϵ and ε' that $Q(\epsilon;\varepsilon')$ is a real and non-negative quantity, $Q(\epsilon;\varepsilon') \geqslant 0$. Introducing the dimensionless variables and parameters [Eq. (8)], one can readily describe in Eq. (9) the integration range $\Omega(z,t)$ including $\Omega(\epsilon = z\nu_0^2, \varepsilon' = t\nu_0^2)$ and $t_1 \leqslant t \leqslant t_2$, as consisting of four two-dimensional ranges

$$t_1 \leqslant t \leqslant t_2,\ z_{\min} \leqslant z \leqslant t_1 - \varsigma,$$

$$t_2 + \delta \leqslant z \leqslant z_{\max}, \tag{A5}$$

$$t_1 - \varsigma \leqslant z \leqslant t_2 - \varsigma, \quad z + \varsigma \leqslant t \leqslant t_2,$$

$$t_1 + \delta \leqslant z \leqslant t_2 + \delta, \quad t_1 \leqslant t \leqslant z - \delta, \tag{A6}$$

where $t_i \equiv \varepsilon_i'/\nu_0^2$ ($i = 1,2$) and ε_i' is defined in Eq. (6). Moreover, the parameter ς is introduced as the lower value of $|t-z|$ for cutting off the divergence of the integral in Eq. (9) and of $q(\epsilon;\varepsilon')$ in Eq. (A4), at $|t-z| \to 0$. The cutoff is meaningful because only the long-wave approximation is relevant for the SMD model (see Sec. III), with $\lambda_{ac} = 2\pi q^{-1}(\epsilon;\varepsilon') = (s/\nu_0)[(t-z+\delta)(t-z)^3]^{1/2} \times [\sqrt{z}(\tau-z)^2 + \tau\delta]^{-1} > R_{av} = a_1 c_{sm}^{-1/3}$. In fact, ς is finite though small, e.g., $\varsigma \approx 0.05$, at a finite

$\delta(>0)$ while $\varsigma=0$ at $\delta=0$. In numerical calculations, typical values of the following parameters are used: $\delta=0.1$, $\nu_0=1$ THz, $c_{sm}=3\times10^{-2}$, and, for sound-wave-like vibrations, $z_{\min}=0$ and $z_{\max}=6$ (e.g., $z_{\max}\approx(2^2-3^2)\nu_{BP}^2\nu_0^{-2}$ (see Ref. 3 and Sec. III) at $\nu_{BP}\simeq\nu_0$. Moreover, the lower limit t_1 for the variable $t\equiv\nu'^2/\nu_0^2$ is estimated with Eq. (6) as $t_1\simeq(3w/h\nu_0)^2\approx0.1$ (Sec. II), while the upper limit t_2 can be estimated from the definition of the typical frequency ν_0 as being the average value for the original bare DOS $g_{sm}^{(0)}(\nu')\propto(\nu')^{\alpha}$, e.g., from $t_2(\nu_0)=1$. One can obtain from Eqs. (6)–(9) and (A3)–(A6) that the dimensionless DOS $\mathbf{J}(u)$ can be described by the expressions in Eqs. (10)–(12).

*Corresponding author. Electronic address: klingem@mail.biu.ac.il

[1] *Amorphous Solids: Low-Temperature Properties*, edited by W. A. Phillips (Springer, Berlin, 1981).
[2] M. I. Klinger, Phys. Rep. **165**, 275 (1988); Philos. Mag. B **81**, 1273 (2001).
[3] G. Ruocco and F. Sette, J. Phys.: Condens. Matter **13**, 9141 (2001).
[4] G. Parisi, J. Phys.: Condens. Matter **15**, S765 (2003).
[5] W. Gotze and M. R. Mayr, Phys. Rev. E **61**, 587 (2000).
[6] J. Horbach, W. Kob, and K. Binder, Eur. Phys. J. B **19**, 531 (2001).
[7] M. I. Klinger and A. M. Kosevich, Phys. Lett. A **280**, 365 (2001); **295**, 311 (2002).
[8] T. S. Grigera, V. Martin-Mayor, G. Parisi, and P. Verrocchio, Phys. Rev. Lett. **87**, 085502 (2001); T. S. Grigera, V. Martin-Mayor, G. Parisi, and P. Verrocchio, Nature (London) **422**, 289 (2003); S. Ciliberti, T. S. Grigera, V. Martin-Mayor, G. Parisi, and P. Verrochio, J. Chem. Phys. **119**, 8577 (2003).
[9] M. I. Klinger and V. Halpern, Phys. Lett. A **313**, 448 (2003).
[10] A. F. Ioffe and A. R. Regel, Prog. Semicond. **4**, 237 (1960).
[11] R. Brout and W. Wisscher, Phys. Rev. Lett. **9**, 54 (1962).
[12] Yu. Kagan and Ya. Iosilevskii, Zh. Eksp. Teor. Fiz. **42**, 259 (1962).[Sov. Phys. JETP **15**, 182 (1962).
[13] V. L. Gurevich, D. A. Parshin, and H. R. Schober, Phys. Rev. B **67**, 094203 (2003).
[14] S. N. Taraskin and S. R. Elliott, Phys. Rev. B **56**, 8605 (1997); Philos. Mag. B **82**, 197 (2002); W. Schirmacher, G. Diezemann, and C. Ganter, Phys. Rev. Lett. **81**, 136 (1998); J. W. Kantelhardt, S. Russ, and A. Bunde, Phys. Rev. B **63**, 064302 (2001).
[15] M. I. Klinger, in *Problems of Modern Physics* (in Russian), edited by A. P. Aleksandrov (Nauka, Leningrad, 1980), p. 293.
[16] M. I. Klinger and V. G. Karpov, Solid State Commun. **37**, 975 (1981); F. N. Ignatiev, V. G. Karpov, and M. I. Klinger, J. Non-Cryst. Solids **55**, 307 (1983).
[17] U. Buchenau, Y. M. Galperin, V. L. Gurevich, D. A. Parshin, M. A. Ramos, and H. R. Schober, Phys. Rev. B **46**, 2798 (1992).
[18] I. M. Lifshits, S. A. Gredescul, and L. A. Pastur, *Introduction to the Theory of Disordered Systems* (Wiley, New York, 1988).
[19] A. M. Kossevich, *The Crystal Lattice: Phonons, Solitons, Dislocations* (Wiley-VCH, Berlin, 1999).
[20] P. W. Anderson, *Concept in Solids* (Benjamin, New York, 1964); *Basic Notions of Condensed Matter Physics* (Benjamin-Cummings, London, 1984).
[21] C. A. Angell, J. Phys.: Condens. Matter **12**, 6463 (2000), and references therein.
[22] P. W. Anderson, B. I. Halperin, and C. M. Varma, Philos. Mag. **25**, 1 (1972); W. A. Phillips, J. Low Temp. Phys. **7**, 351 (1972).
[23] R. Shuker and R. W. Gammon, Phys. Rev. Lett. **25**, 222 (1970).
[24] N. V. Surovtsev and A. P. Sokolov, Phys. Rev. B **66**, 054205 (2002).
[25] S. Kojima and M. Kodama, Physica B **263-264**, 336 (1999); Y. Inamura, M. Arai, O. Yamamuro, A. Inaba, N. Kitamura, T. Otomo, T. Matsuo, S. M. Bennington, and A. C. Hannon, Physica B **263-264**, 299 (1999).
[26] T. Achibat, A. Boukenter, and E. Duval, J. Chem. Phys. **99**, 2046 (1993).
[27] N. V. Surovtsev, J. A. H. Wiedersich, V. N. Novikov, E. Rossler, and A. P. Sokolov, Phys. Rev. B **58**, 14888 (1998); J. Wiedersich, N. V. Surovtsev, V. N. Novikov, E. Rossler, and A. P. Sokolov, *ibid.* **64**, 064207 (2001); V. N. Novikov, A. P. Sokolov, B. Strube, N. V. Surovtsev, E. Duval, and A. Mermet, J. Chem. Phys. **107**, 1057 (1997); A. P. Sokolov, E. Rossler, A. Kisliuk, and D. Quitmann, Phys. Rev. Lett. **71**, 2062 (1993).
[28] S. Hunklinger and A. K. Raychaudhari, in *Progress in Low Temperature Physics IX*, edited by D. F. Brewer (Elsevier, Amsterdam, 1986), p. 265.
[29] W. Heitler, *The Quantum Theory of Radiation* (Clarendon Press, Oxford, UK, 1954).
[30] A. Matic, D. Engberg, C. Masciovecchio, and L. Borjesson, Phys. Rev. Lett. **86**, 3803 (2001); A. Matic, L. Borjesson, G. Ruocco, C. Masciovecchio, A. Mermet, F. Sette, and R. Verbeni, Europhys. Lett. **54**, 77 (2001).